

Cascade Polymeric MRI Contrast Media Derived from Poly(ethylene glycol) Cores: Initial Syntheses and Characterizations

YanJun Fu,* Hans-Juergen Raatschen, Danute E. Nitecki, Michael F. Wendland, Viktor Novikov, Laure S. Fournier, Clemens Cyran, Victor Rogut, David M. Shames, and Robert C. Brasch

Center for Pharmaceutical and Molecular Imaging, Department of Radiology, University of California San Francisco (UCSF), 513 Parnassus Avenue, San Francisco, California 94143-0628

Received December 1, 2006; Revised Manuscript Received January 26, 2007

Diagnostic contrast media for magnetic resonance imaging (MRI) are often applied to enhance the signal of blood allowing for quantitative definition of vascular functional characteristics including tissue blood volume, flow, and leakiness. Well-tolerated and safe macromolecular formulations are currently being sought that remain in the blood for a relatively long period and that leak selectively from diseased vessels, particularly cancer vessels. We synthesized a new class of macromolecular, water-soluble MRI contrast media by introducing two diverging polylysine cascade amplifiers at each end of a poly(ethylene glycol) (PEG) backbone, followed by substitution of terminal lysine amino groups with Gd–DTPA chelates. Four candidate PEG cascade conjugates are reported here, PEG3400-Gen4-(Gd–DTPA)₈, PEG6000-Gen4-(Gd–DTPA)₈, PEG12000-Gen4-(Gd–DTPA)₈, and PEG3400-Gen5-(Gd–DTPA)₁₃ with descriptions of their basic physical, biological, and kinetic properties, including real and effective molecular sizes, proton T1 relaxivities in water and plasma, partition coefficients, osmolalities, chelate stability, stability in plasma, stability to autoclaving, certain in vivo pharmacokinetics (blood half-life, blood clearance, volume of distribution), and whole body elimination profiles in normal rodents. These candidate PEG-core cascade MRI contrast media showed a range of effective molecular sizes similar to proteins weighing 74–132 kDa, although their actual molecular weights were much smaller, 12–20 kDa. All compounds exhibited a narrow range of size dispersity and relatively high T1 relaxivities (approximately 3 times the value for unconjugated Gd–DTPA at 2 T and 37 °C). Representative compounds also showed a high degree of hydrophilicity, stability in solution buffer and plasma, and lack of binding to proteins. The two candidate compounds with the largest effective molecular sizes, PEG12000-Gen4-(Gd–DTPA)₈ and PEG3400-Gen5-(Gd–DTPA)₁₃, had longer blood half-lives, 36 and 73 min, respectively (monoexponential kinetics for both), and showed strong, prolonged MRI enhancement of vessels. Results also indicate that in vivo pharmacokinetics and bodily elimination profiles can be adjusted by the selection of molecular size for the PEG core and the selection of the amplification degree of the cascade polylysine clusters. The initially evaluated compounds from this new class of contrast media show acceptable, desirable characteristics in many, but not all, respects. Further efforts are directed toward candidate macromolecules having higher thermodynamic stability, higher degree of substitution by gadolinium chelates, and more rapid bodily elimination.

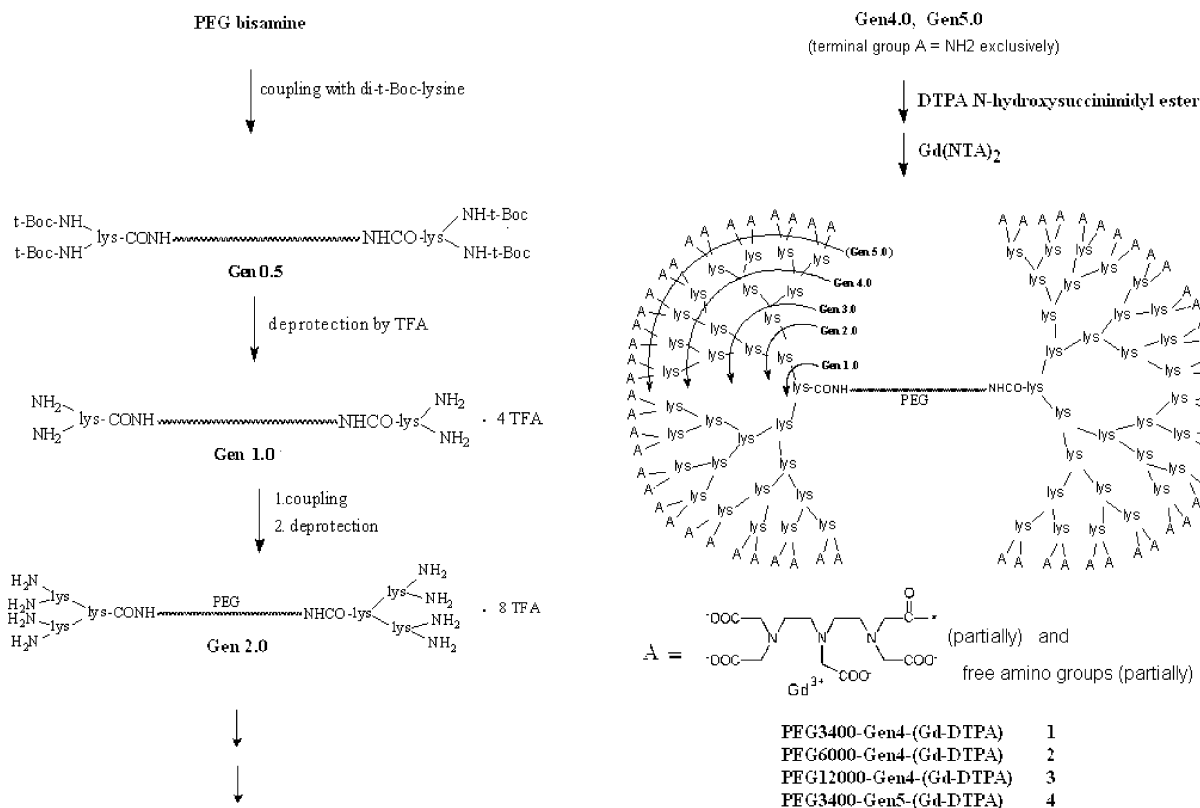
Introduction

Intravenously administered image contrast-enhancing drugs, often called “contrast media”, are used frequently in the clinical practice of magnetic resonance imaging (MRI) to aid in the identification and characterization of diseases. Because their purpose is enhanced diagnosis rather than disease therapy, contrast media are held to a particularly high standard of safety. With few exceptions, all currently used MRI contrast media are less than 1000 Da in molecular weight (e.g., Gd–DTPA, Gd–DOTA, Gd–HP-DO3A) and belong to the class of small molecular contrast media (SMCM). After intravascular administration they rapidly distribute throughout the extracellular fluid space, exclusive of the normal central nervous system, a pattern sometimes called a “nonspecific” distribution but which, as such, has proven highly useful.¹ A primary and particularly valuable application of these SMCM has been to highlight disruptions

of the blood–brain barrier. However, contrast media having different pharmacokinetic and distribution patterns, particularly a blood pool, intravascular distribution, have been proposed as being superior to SMCM for certain applications.² Unique advantages attributed to blood pool contrast media, formulated as macromolecules, include potential to quantitatively measure vascular characteristics such as blood volume and abnormal transendothelial leakiness (or hypermeability), particularly outside the central nervous system. A prolonged angiographic effect is a useful secondary effect of macromolecular agents. These potentials, quantitative microvessel characterization and prolonged angiographic effect, have particular appeal for cancer imaging evaluations.

Multiple macromolecular contrast media (MMCM) formulations have been proposed and tested, establishing in preclinical investigations their unique diagnostic potential, as recently reviewed by Daldrup-Link and Brasch³ and by Kobayashi and Brechbiel,⁴ but no MMCM has demonstrated all the desirable characteristics to be successfully advanced to governmental

* Corresponding author. Phone: (415) 476-4329. Fax: (415) 476-5595. E-mail: yanjun.fu@radiology.ucsf.edu.

Scheme 1. Synthesis of Gd-Based Cascade Polymeric MRI Contrast Media with PEG Cores

approval and clinical practice. Problems encountered differ with the candidate MMCM being tested but include too small a molecular size to differentiate leakiness of cancer vessels from nonleaky normal vessels, high polydispersity of product, instability, poor tolerance, incomplete elimination, and coexisting protein-bound and unbound forms that make kinetic analysis difficult.

In this report we describe the initial syntheses and characterizations of candidate compounds from a new class of MMCM consisting of a PEG core and two peripheral Gd-containing cascade polymer amplifiers. This novel arrangement of commonly used, hence substantially tested and biocompatible, components (PEG, cascade polylysine, Gd chelates) allows for macromolecular contrast media formulation in a desirable range of sizes and conformations.

Experimental Section

Materials and Apparatus. Poly(ethylene glycol) bisamine 3400 (M_n 3290, M_w 3321, polydispersity index 1.01) was purchased from Shearwater Polymers Inc. Poly(ethylene glycol) (PEG) 6000 (M_n 6470, M_w 6517, polydispersity index 1.01, measured by MALDI-TOF mass spectrometry) was purchased from Fluka. PEG12000 (M_n 12163, M_w 12 650, polydispersity index 1.04 according to the manufacturer's data) was purchased from Polymer Labs. These PEGs or PEG bisamine were dried by azeotropic distillation with anhydrous benzene before subsequent derivatization. N^2,N^6 -di-*t*-butyl-oxycarbonyl-L-lysine dicyclohexylamine salt (N^2,N^6 -di-*t*-Boc-L-Lys-DCHA) was purchased from Advanced ChemTech, diethylenetriamine-pentaacetic acid (DTPA) was purchased from Fluka, gadolinium chloride hexahydrate and nitrilotriacetic acid (NTA) were obtained from Aldrich. Other chemicals were from Aldrich, Sigma, or Fischer Scientific. All these reagents were of analytical grade or superior.

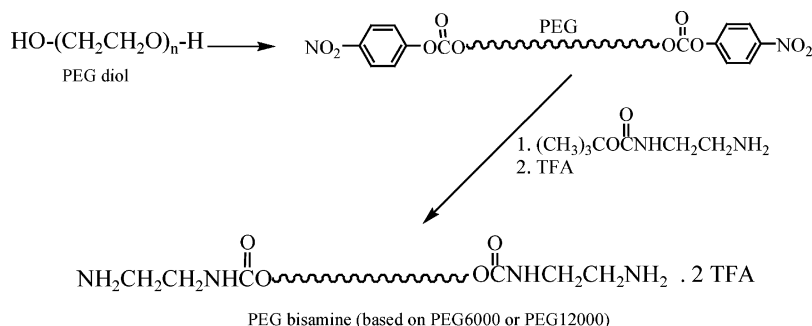
Analytical size exclusion (SE)-HPLC was performed on a Superdex 200 10/300 GL column (10 mm \times 300 mm, Amersham Biosciences, Uppsala, Sweden) using a Rainin HPLC system (Rainin Instrument

Inc., Emeryville, CA) with a Knauer diode array UV detector (210 nm) and a Shimadzu RID-6A as refractive index detector. Preparative size exclusion chromatography (SEC) was performed on Sephadex G-75 and G-100 columns (5 cm i.d. \times 50 cm) with UV detection at 214 nm. ¹H NMR spectra were recorded on a Varian 400 NMR spectrometer. MALDI-TOF mass spectra were obtained on a Perkin-Elmer Voyager DESTRA mass spectrometer. Gd analysis was conducted using inductively coupled plasma atomic emission spectrometry (ICP-AES) and inductively coupled plasma mass spectrometry (ICP-MS) (Huffman Labs, Golden, CO). Elemental analysis was conducted by Schwarzkopf Microanalytical Lab (Woodside, NY). UV measurements were conducted on a Shimadzu UV-260 spectrophotometer. Proton relaxivity measurements were conducted at a 0.25 T PRAXIS II relaxometer and a 2 T Omega CSI-II MR imager (Bruker, Fremont, CA). Dialysis was conducted using the regenerated cellulose Spectra/Por tubing (cutoff MW 3500 Da).

Twenty-four Sprague-Dawley rats (female, age 4–5 weeks, 90–100 g, Harlan, Indianapolis, IN) were used for blood pharmacokinetic studies ($n = 18$) and whole body clearance studies ($n = 6$), respectively.

Synthesis of PEG-Core Cascade Polylysines. Four different PEG-based cascade polymers with unmodified amino groups were synthesized according to a previously described method, including PEG3400-Gen4, PEG6000-Gen4, PEG12000-Gen4, and PEG3400-Gen5.⁵ Generally, the PEG diol (6 or 12 kDa) was converted to PEG bisamine, via the reaction of PEG bis(4-nitrophenyl carbonate) with excess 1-*N*-*t*-butyloxycarbonyl(Boc)-ethylenediamine followed by *t*-Boc deprotection in trifluoroacetic acid (TFA). PEG3400 bisamine was purchased from Shearwater Polymers, Inc. PEG bisamine (also termed "generation 0", or abbreviated "Gen0") was conjugated with excess carboxy species, N^2,N^6 -di-*t*-Boc-L-lysine, via dicyclohexylcarbodiimide coupling method; the resulting *t*-Boc-protected half-generation cascade polymer (Gen0.5) was deprotected by TFA to give Gen1.0 cascade polymer. This coupling-deprotection cycle was repeated again and again, to yield progressive generations of cascade polymers. (Schemes 1 and 2). With the increase of the cascade polymer generation, the reaction time and excess amount of monomer di-*t*-Boc-L-lysine in the coupling step have to be increased. Meanwhile, to ensure the complete capping of polymer

Scheme 2. Conversion of a PEG Diol to a Corresponding PEG Bisamine as the Starting Molecule in the Synthesis of PEG-Core Cascade Polymers



amino groups, ninhydrin test and MALDI-TOF mass spectrometry were used to monitor the completeness of the coupling reaction. Synthesized PEG-core cascade polylysines were then purified by dialysis in distilled water. As necessary in some cases, preparative SEC (Sephadex G-75) was also applied (mobile phase: 0.1 M trifluoroacetate buffer with pH 3.0) for further purification. Synthesized PEG-based cascade polymers were characterized by ^1H NMR, MALDI-TOF mass spectrometry, and amino quantification. Their purity was confirmed by SE-HPLC on a Superdex 200 10/300 GL column (Amersham Biosciences), with a solution of 0.1% TFA and 0.3 M Na_2SO_4 (pH 2.7) as the mobile phase at 0.80 mL/min flow rate and 23 °C (UV detection at 210 nm). DMF was generally chosen as the solvent in the coupling steps, but methylene chloride worked well as a reaction medium for lower generation cascade polymers (<generation 3). A mixture of methylene chloride and TFA (1:1) was always used as the deprotection reaction medium. Yields in each cycle ranged from 85% to 92% (coupling step) and 90–98% (deprotection step), respectively.

PEG3400-Gen4, PEG6000-Gen4, PEG12000-Gen4, and PEG3400-Gen5 polymers, respectively, were found to have actual molecular weights of 7.4, 10.3, 16.8, and 11.3 kDa, with terminal amino numbers of 32.5, 32.1, 31.6, and 61.2. Their polydispersity indices (PDI) in molecular weight were all less than 1.03. Elemental analysis gave expected results for purified cascade polymers. For those full generation cascade polymers with the generation <4, a classic trinitrobenzene sulfonic acid (TNBS) method was used to determine the content of primary amino groups.⁶ For cascade polymers with higher generations, a potentiometric acid–base titration method was used to quantify their amino group contents.⁷ The titration was conducted manually using a Corning model 125 pH meter and an Aldrich pH electrode at room temperature (23 °C). Briefly, about 100 mg (approximately 0.1–0.4 mmol of amino group) of a cascade polymer (as the TFA salt of the polyamine) was dissolved in 10 mL of degassed 0.1 M NaCl solution, then titrated by 19.4 mM NaOH to pH 11. The turning points at pH were determined from the titration curve. The amount of amino groups of the sample was calculated from the determined titrant volume and its concentration.

DTPA Conjugation to Amino Termini of PEG-Core Cascade Polymers Followed by Chelation with Gadolinium Ions. DTPA *N*-hydroxysuccinimidyl ester (DTPA-ONSu) was prepared as follows: DTPA (10 mmol, 3.93 g) was dissolved in DMF (20 mL) in the presence of diisopropylethylamine (50 mmol, 6.45 g). Cooled to 0 °C, to this solution were added *N*-hydroxysuccinimide (NSu-OH, 5 mmol, 0.58 g) and dicyclohexylcarbodiimide (5 mmol, 1.03 g). After 24 h at room temperature, the mixture was filtered, giving a DMF solution containing 5 mmol of the active ester.

The PEG-core cascade polymer sample (1 mmol NH_2 contained) was dissolved in 15 mL of HEPES buffer solution (0.1 M, pH 8.2) and cooled to 5 °C. DTPA-ONSu (5 mmol) solution in DMF prepared above was added slowly at this temperature over 20 min. The mixture was stirred for a further 0.5 h at 5 °C and then for 24 h at room temperature. The resulting solution was dialyzed against distilled water (3×2 L) to remove excess DTPA. Two conjugates, PEG6000-Gen4-DTPA and PEG3400-Gen5-DTPA, were further purified by SEC

Table 1. Chemical Data of Representative PEG3400-Core Cascade Polymers as Free Amines

cascade polymer	calculated M_n	measured ^a			no. of amino groups	
		M_n	M_w	PDI M_w/M_n^a	theor	measured
Gen0.0	3290	3290	3321	1.009	2	2.0 ^b
Gen2.0	4059	4105	4134	1.007	8	7.9 ^b
Gen3.0	5083	5149	5159	1.002	16	16.9 ^b (16.2) ^c
Gen4.0	7133	7369	7390	1.003	32	32.5 ^c
Gen5.0	11232	11328	11339	1.001	64	61.2 ^c

^a The molecular weight of the cascade polymer was measured by MALDI-TOF mass spectrometry. M_n is the number-average molecular weight, M_w is the weight-average molecular weight, and PDI is the polydispersity index. ^b Measured by the trinitrobenzene sulfonic acid (TNBS) method. ^c Measured by the acid–base titration method.

(mobile phase: 0.05 M HEPES and 0.15 M NaCl at pH 7.0) and used specifically for Gd chelation stability measurements. Gd(NTA)₂ solution (100 mM, 15 mL) was mixed with the dialyzate at pH 5.0–5.5 for 24 h. After the trans-chelation, the reaction mixture was adjusted to pH 7 and dialyzed to remove excess Gd(NTA)₂ and released NTA, giving a crude product which was shown to be negative in an arsenazo III test.

Purification and Chemical Characterization of Synthesized Contrast Media. The dialyzate obtained above was concentrated by rotary evaporation to 5 mL and underwent preparative size exclusion chromatography (Sephadex G-100, 5 cm i.d. \times 50 cm column) with 0.15 M NaCl and 0.05 M HEPES (pH 7.0) as the mobile phase (flow rate 12 mL min⁻¹ cm⁻²). Fractions were monitored at 214 nm. The major peak fractions in the macromolecular range were pooled and then dialyzed against distilled water (2×2 L) to remove the buffer salts. Finally, the dialyzate was lyophilized to give a white, loose material as the Gd-DTPA conjugated polymers (compounds 1–4, Tables 2 and 3), as pure products. Yields ranged from 74% to 87% based on the PEG component. These chromatographically pure polymeric contrast media were further characterized by Gd analysis (ICP-AES), with their chemical composition confirmed by routine elemental analysis. Further, the number of covalently attached Gd-DTPA and actual molecular weight of each contrast medium were calculated based upon the result of the Gd analysis, which agreed well with the elemental analysis results.

The purity of final products was confirmed by analytical SE-HPLC on a Superdex 200 10/300 GL column. A solution of 0.05 M phosphate and 0.15 M NaCl (pH 7.0) was used as the mobile phase at 0.80 mL/min flow rate and 23 °C (210 nm).

Effective Molecular Weight Measurements by SE-HPLC. With the same SE-HPLC column, a molecular weight calibration curve was created based on HPLC measurements of five protein standards (listed in increasing order of MW: cytochrome *c*, carbonic anhydrase, bovine serum albumin, alcohol dehydrogenase, and amylase) with molecular weights of 13, 29, 66, 150, and 200 kDa, respectively. The size distribution of each Gd-based polymer, represented by the polydispersity index (PDI), was calculated by the following equation: $\text{PDI} = M_w/M_n$

Table 2. Chemical and Physicochemical Properties of PEG-Core Macromolecular MRI Contrast Media^a

contrast medium	polydispersity (M_w/M_n)	Gd % (w/w)	MW (kDa) ^b		chelation stability (log K) ^c	hydrophilicity ($\times 10^{-5}$) ^d	osmolality	
			actual	effective			mole Gd/L	mOsm/kg H ₂ O
PEG3400-Gen4-(Gd-DTPA) ₈	1.03	10.70	12.2	74	nd	1.0 \pm 0.1	0.1	389 \pm 8
PEG6000-Gen4-(Gd-DTPA) ₈	1.04	8.31	14.2	82	18.3 \pm 0.2	nd	0.1	407 \pm 11
PEG12000-Gen4-(Gd-DTPA) ₈	1.05	6.26	20.1	132	nd	<0.8	0.1	462 \pm 8
PEG3400-Gen5-(Gd-DTPA) ₁₃	1.04	11.02	18.4	106	18.6 \pm 0.2	nd	0.1	604 \pm 13
albumin-Gd-DTPA) ₃₅	nd	5.98	92	180	18.8 \pm 0.1 ^e	28.0 \pm 1.8	0.1	806 \pm 16
Gd-DTPA (Magnevist)	na	28.75	0.6	na	22.3 ^f	2 ^f	0.5	1940 ^f

^a The mean \pm standard error was given for measures of thermodynamic stability, hydrophilicity, and osmolality. ^b Effective MWs were determined by SE-HPLC. ^c Logarithm value of the thermodynamic stability constant (K). ^d Partition coefficient between 1-butanol and 50 mM HEPES buffer (pH 7.4). ^e Literature data (ref 11). ^f Literature data (ref 44).

Table 3. Proton Relaxivities and Blood Pharmacokinetics for PEG-Core Cascade Macromolecules with Comparable, Previously Characterized Gadolinium-Based MRI Contrast Media

contrast medium	effective MW (kDa)	blood pharmacokinetic parameters, mean (SD) ^b			
		$t_{1/2}$ (min)	V_d (L/kg)		Cl mL/(min kg)
			V_c	V_{ss}	
PEG3400-Gen4-(Gd-DTPA) ₈ ^a	74	3.0 (0.5) α 22.6 (6.7) β	0.089 (0.004)	0.180 (0.010)	5.27 (1.66)
PEG6000-Gen4-(Gd-DTPA) ₈ ^a	82	5.9 (0.6) α 40.2 (15.6) β	0.054 (0.005)	0.117 (0.011)	3.67 (1.71)
PEG12000-Gen4-(Gd-DTPA) ₈	132	35.7 (6.7)	0.154 (0.064)		2.79 (0.57)
PEG3400-Gen5-(Gd-DTPA) ₁₃	106	72.6 (4.9)	0.084 (0.004)		0.79 (0.09)
albumin-(Gd-DTPA) ₃₅	181	250.9 (17.6) ^c	0.046 (0.006) ^c		0.15 (0.02) ^c
Gd-DTPA	na	13.1 (2.4) ^c β	na	0.242 (0.034) ^c	14.3 (3.9) ^c

^a For PEG3400-Gen4-(Gd-DTPA)₈ and PEG6000-Gen4-(Gd-DTPA)₈, blood half-lives data were presented as mean \pm error. ^b $t_{1/2}$ stands for blood half-life (α and β refer to distribution and elimination phases, respectively, for biexponential kinetics), V_d is the volume of distribution, V_c is the distribution volume of the central compartment, V_{ss} is the steady-state distribution volume, and Cl is the total clearance rate. ^c See literature data (ref 45).

$= (\sum N_i M_i^2 / \sum N_i M_i) / (\sum N_i M_i / \sum N_i)$, M_w and M_n are weight- and number-average molecular weights, respectively, while N_i and M_i stand for the molecular number and molecular weight, respectively, of the i th fraction of a macromolecular sample.

Formulation of Contrast Media and Their Autoclaving Stability. Calculated amounts of lyophilized contrast media were dissolved in distilled water, yielding concentrations of 0.1 M with respect to Gd(III). The resulting solutions were sterile filtered twice with Acrodisc 25 mm syringe filters (0.2 μ m, Gelman Laboratory) and stored at 0–5 °C. In practical imaging experiments, these solutions were diluted to ~20 mM Gd for animal intravenous injections. The pH values of formulated contrast media were in the range of 6.6–7.4. One chosen contrast medium, PEG3400-Gen5-(Gd-DTPA)₁₃ at 0.1 M concentration, was autoclaved for 30 min at 120 °C, followed by SE-HPLC measurement to see if decomposition occurred.

Proton T1 Relaxivity Measurements. For each synthesized contrast medium, T1 relaxation times for sample solutions in 0.1 M HEPES buffer (pH 7.4) with known Gd concentrations were measured. The measurements were conducted at the magnetic field of 0.25 or 2.0 T and at room temperature (23 °C) or physiological temperature (37 °C). At 0.25 T (PRAXIS II relaxometer), T1 relaxation times of sample solutions were determined by the saturation–recovery method (90– τ –90 sequence, 32 incremental τ values) using monoexponential fittings with a linear, least-squares regression (in all cases the correlation coefficients >0.998).⁸ At 2.0 T (Bruker CSI-II superconducting MR imager), sample T1 time measurements were conducted using an inversion–recovery method (180– τ –90 sequence) with a fixed TR (3000 ms) and 16 varying TI (50, 250, 450, 650, 850, ..., 3050 ms).⁹ T1 data were obtained by a monoexponential fitting (correlation coefficients >0.996). Plasma solutions of all contrast media, as well as blank plasma, were tested for T1 measurement at 0.25 T and 37 °C.

Thus, a series of dilute contrast medium solutions (ca. 0.1, 0.2, 0.5 mM Gd) of each contrast medium was tested, as well as the blank HEPES solution and rat plasma. T1 relaxivity of tested contrast medium in buffer solution or plasma was calculated by a linear fitting of the

observed T1-versus-concentration curve (correlation coefficients >0.998). Compounds **1** and **4** were selected for evaluation of stability in plasma by performing repeated T1 relaxation measurements in the same plasma solution over 72 h at 37 °C.

Hydrophilicity, Osmolality, and Chelation Stability. The hydrophilicity as reflected by the butanol–water partition coefficients of representative compounds, PEG3400-Gen4-(Gd-DTPA)₈ and PEG12000-Gen4-(Gd-DTPA)₈, was measured using a flask-shaking method¹⁰ as used by Krause et al.; albumin-(Gd-DTPA)₃₅ was also tested for comparison. Each compound was assayed in duplicate. HEPES buffer (50 mM, pH 7.4) and 1-butanol were chosen as two immiscible solvents. The contrast medium was dissolved in HEPES buffer. A volume of 8 mL of a contrast medium solution was mixed with 8 mL of 1-butanol and shaken for half an hour in a separation funnel (30 mL). After centrifugation, the water phase and butanol phase were separated. After acid digestion (reflux in concentrated nitric acid), the Gd concentrations in both phases, C1 (aqueous phase) and C2 (butanol), were determined using the highly sensitive ICP-MS technique (detection limit as low as 1 ppb). The partition coefficient, represented as the ratio of C2/C1, was thus calculated.

Osmolality values of all synthesized contrast media were measured at 0.1 M Gd solutions using a conventional freezing point depression method on a wide-range osmometer (model 3W, Advanced Instruments, Needham Heights, MA), expressed with a unit of “mOsm/kg water”. The osmometer was calibrated with standard NaCl solutions (100 and 900 mOsm/kg water) before sample measurements. Each sample was measured in duplicate.

Gd chelation stability was studied according to an established method through competitive Gd³⁺ chelation¹¹ between the indicator arsenazo III and two chosen polymeric ligands, PEG6000-Gen4-DTPA and PEG3400-Gen5-DTPA. Briefly, first the conditional stability constants were determined in a pH 4.0 buffer (0.01 M acetate and 0.1 M NaCl), by titrating a solution of known total concentrations of Gd(III) and arsenazo III with the competing ligand in a UV spectrophotometric cuvette; the change in the absorption at 660 nm was monitored at room

temperature. A single titration process was completed until the competing equilibrium was reached in 15–20 min, when no further change was observed in the absorption. The pH 4 conditional stability constant was thus calculated for each compound according to theoretical equations in the literature. Second, their thermodynamic stability constants were further calculated, assuming the stepwise protonation constants of these polymeric DTPA monoamide ligands are the same as those of a DTPA monopropylamide.¹¹

Blood Pharmacokinetic Study. Healthy Sprague–Dawley rats (female, 4–5 weeks old, 90–100 g) were randomly divided into four groups for blood pharmacokinetic measurements by dynamic MRI enhanced with four synthesized contrast media ($n = 4$ or 5 per group, total = 18) on a 2 T Omega CSI-II MR imager. Animal experiments were performed in accordance with the institutional Guide for the Care and Use of Laboratory Animals with approval from the Committee for Animal Research. Animals were anesthetized by a combined intraperitoneal injection of sodium pentobarbital (35 mg/kg) and buprenorphine hydrochloride (0.025 mg/kg) and placed supine in the magnet within a birdcage radio frequency coil. The change in relaxation rate, $(1/T1)_{\text{post}} - (1/T1)_{\text{pre}}$, in the blood of the vena cava over time (50–70 min) was measured noninvasively by dynamic MRI using a three-dimensional spoiled gradient refocusing sequence (3D-SPGR) for each animal and each contrast medium group according to a previously published method.^{12,13} Since the contrast-induced $1/T1$ change is assumed to be directly proportional to the Gd concentration under the experimental conditions, this $\Delta(1/T1)$ -versus-time curve is essentially the blood concentration-versus-time curve for each contrast medium.^{12,13} Blood pharmacokinetic parameters including blood half-life ($t_{1/2}$), volume of distribution (V_c and V_{ss} , specifically, distribution volume of central compartment and distribution volume of the combined central and periphery compartments, respectively), and total blood clearance (Cl) were thus calculated for each contrast medium group using a conventional two-compartmental model.¹⁴ The dose of each macromolecular contrast medium was 40 μmol Gd/kg body weight.

Whole Body Clearance. Six Sprague–Dawley rats (Harlan, Indianapolis, IN) were randomly divided into two equal groups for preliminary whole body clearance studies of two selected macromolecular contrast media, **3** and **4** ($n = 3$ each). Animals were put into metabolic cages immediately after intravenous contrast medium injection (40 μmol Gd/kg) for 1–3 weeks. At sacrifice time, the liver, both kidneys, and remaining carcass for each animal were collected. Rat liver, kidney, and carcass samples were transferred in entirety into glass tubes or beakers and weighed, then thermally charred followed by mixed acid digestion with concentrated nitric acid then concentrated refluxing perchloric acid to fully oxidize all organic material. Resulting digestion solutions were diluted to a final volume of 20.0 mL (for liver or kidney samples) or 500.0 mL (for carcass samples) with deionized water. All resulting solutions were subjected to Gd analysis by ICP-AES and the more sensitive ICP-MS when required.¹⁵

Results and Discussion

Molecular Design and Synthesis of New Contrast Media.

PEG was selected as the backbone of the macromolecular contrast media in our synthesis (Scheme 1) because of its flexibility in molecular size choices and, more importantly, because of its unique ability to strongly bind water molecules via hydrogen bonds, conferring an unusually large hydrodynamic size relative to molecular weight. PEG, buffered by the large quantities of water molecules bound to its surface, tends to exclude all other macromolecules and remains “unseen” by the body’s immune system.¹⁶ Attachment of PEG to proteins or other substituents, making them “stealth”, can prolong the blood half-life of macromolecules while substantially reducing immunogenicity.¹⁶ PEG is readily available in different sizes, relatively inexpensive, and nearly monodisperse (polydispersity index namely $PDI \leq 1.030$).¹⁷ PEG has been incorporated into

macromolecular drugs for human use as early as 1990; the PEG conjugate to adenosine deaminase (ADA), namely, Adagen, has been FDA-approved for clinical use to treat ADA-deficient severe combined immunodeficiency syndrome for more than 1 decade.¹⁸

Because PEG has only two terminal amino groups available for derivatization, a dual amplifying strategy was adopted capable of producing a large number of reactive groups for conjugation with the numerous signal-enhancing groups at both PEG termini desired for dose efficient contrast enhancement. Via stable amide linkages, cascade polylysines with adjustable generations were introduced stepwise to the two ends of PEG bisamine through *t*-Boc chemistry. Park and co-workers reported on their synthesis of cascade polylysines (up to four generations) at one end of methoxy PEG (5 kDa) or both ends of PEG (3.4 kDa) via more expensive fluorenylmethoxycarbonyl (Fmoc) chemistry, for applications in nonvirus in vitro gene delivery as polycation vectors,^{19,20} not as imaging contrast enhancers for in vivo use. Our gadolinium-chelated PEG-core cascade polymers are further chemically modified compared with those reported polymers, not only different in the major synthetic approaches but also different in purpose, used here as MRI contrast medium. Furthermore, both varying the generation of the cascade and the size of PEG core were considered in this study (Scheme 1).

Detailed chemical structure information for PEG-3400 cascade polymers with varying generations is shown in Table 1 and Figure 1 as examples; further information can be found in our recent work.⁵ MALDI-TOF mass spectrometry confirmed that each generation of synthesized cascade polymers had the expected molecular weight and narrow molecular weight distribution.

The subsequent conjugation of cascade polymers with the DTPA ligands was conducted using a conventional DTPA *N*-hydroxysuccinimidyl (NSu-OH) monoester method, followed by the chelation with Gd^{3+} ions. To reduce the risk of the cross-linking, an equivalent ratio of 10:1 between COOH and NSu-OH was adopted. When the feed molar ratio, [active ester]/[amino] was set at 5, approximately 25% and 21% amino substitutions were obtained for generation-4 and generation-5 polymers. Likely, the main reasons for the observed modest substitution include the unwanted hydrolysis of the resulting DTPA-ONSu ester in aqueous buffer and the inherent steric hindrance on the surface of cascade amplifiers. The steric hindrance effect increases when the number of cascade generation increases. One other possible reason for incomplete substitution might be that the initially attached DTPA moieties, having negative charges, may tend to electrostatically repulse those nonattached, also negatively charged, reactive DTPA-ONSu molecules.

The PEG6000-Gen4 polymer was tested to determine the different substitution efficiency caused by the varying feed ratio of [active ester]/[amino]. Similar to the other Gen4 polymer, ~25% of PEG6000-Gen4 amino groups were substituted when this feed ratio equaled 5. When the feed ratio decreased to 3, the substitution percentage declined to 18%; when the feeding ratio increased to 8, the substitution percentage was still only 26%. Thus, the feed molar ratio of [active ester]/[amino] in our standard protocol was selected to be 5. The substitution percentage here referred to the ratio of attached Gd-DTPA to all available amino groups. Under our synthetic conditions, >50% molar excess of $\text{Gd}(\text{NTA})_2$ was added to undergo trans-chelation with the polymer-DTPA conjugate at an appropriate pH (~5.5) and room temperature for a sufficient reaction time

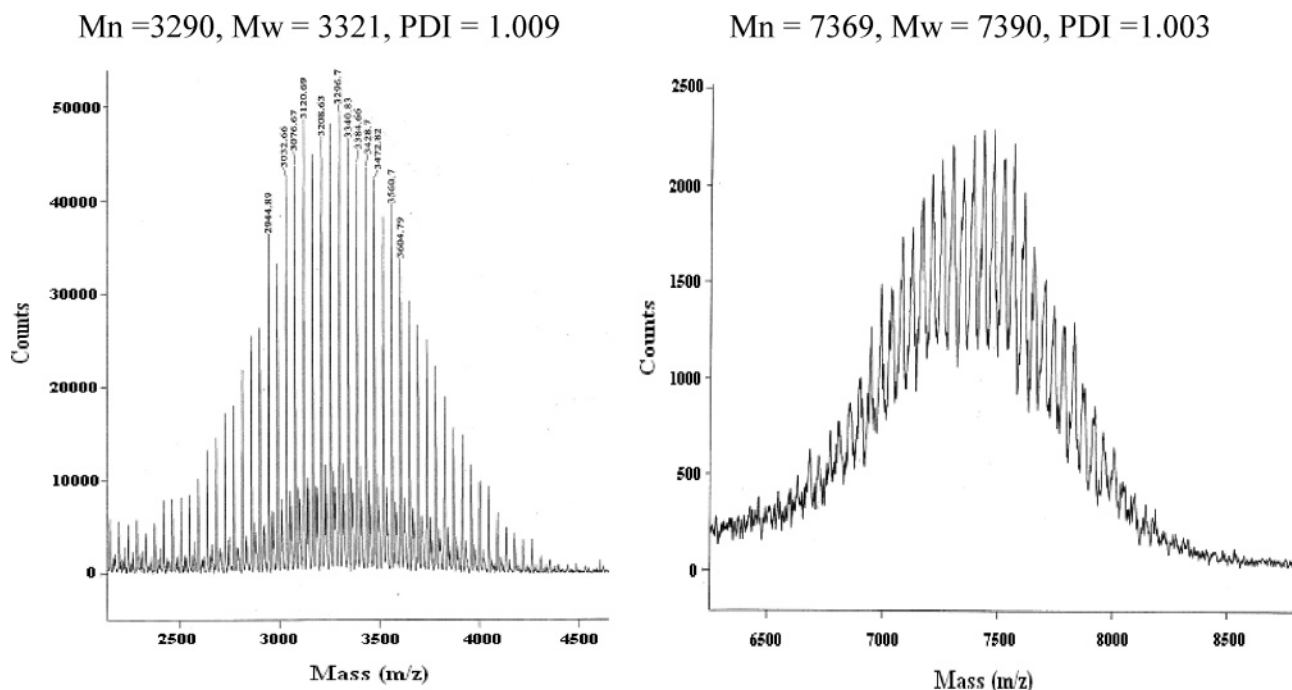


Figure 1. MALDI-TOF mass spectrum of PEG3400 bisamine (left) and PEG3400-amide-Gen4.0 conjugate (right); their calculated polydispersity index (PDI) data were given.

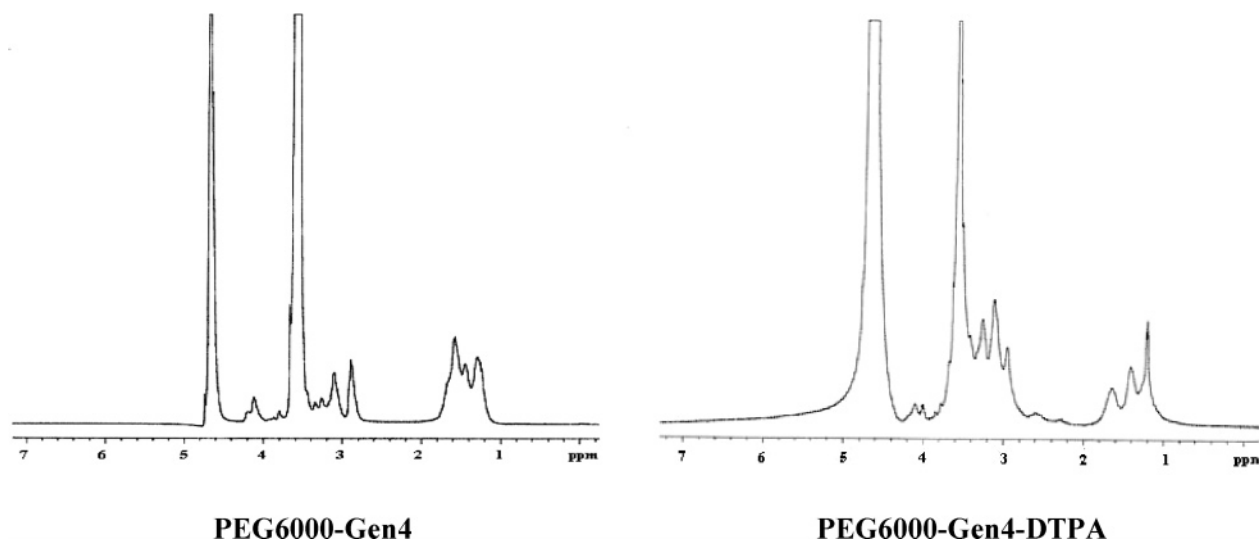


Figure 2. ^1H NMR spectra of PEG6000-Gen4 cascade polymer (free amine) and PEG6000-Gen4-DTPA ligand in D_2O .

(24 h). Further addition of either $\text{Gd}(\text{NTA})_2$ or GdCl_3 in the reaction buffer gave a constant Gd content (e.g., 8.3% as a weight percentage for compound **2**). This indicated that the covalently attached DTPA ligands were completely complexed with Gd^{3+} ions.

The covalent attachment of DTPA was directly evidenced by the NMR spectra of an SEC-purified macromolecular ligand. Figure 2 shows two NMR spectra of PEG6000-core derivatives. Specifically, ^1H NMR (ppm, 400 MHz, in D_2O): for PEG6000-Gen4 cascade polymer, 1.2–1.8 (m, trimethylene group in lysine), 2.8–3.2 (m, CH_2CH in lysine), 3.58 (s, PEG unit $\text{CH}_2\text{CH}_2\text{O}$), 4.0–4.25 (m, CH_2CH in lysine); for PEG6000-Gen4-DTPA conjugate, 1.1–1.8 (m, trimethylene group in lysine), 2.8–3.35 (m, CH_2CH in lysine, $\text{NCH}_2\text{CH}_2\text{N}$ and NCH_2CO groups in DTPA), 3.58 (s, PEG unit $\text{CH}_2\text{CH}_2\text{O}$), 3.95–4.25 (m, CH_2CH in lysine). The number of conjugated DTPA, specifically 7.6 in this example, was calculated from the integral ratio of hydrogen atoms in the DTPA moiety and characteristic

trimethylene groups of lysine residues. This result agreed well with the number of Gd ion measured by ICP-AES for the corresponding contrast macromolecule **2**.

All four synthesized contrast media were purified by preparative size exclusion chromatography. They demonstrated relatively high levels of size monodispersity (1.03–1.05), large effective MWs ranging from 74 to 132 kDa, as anticipated with the PEG core (in contrast to actual MWs that ranged from 12 to 20 kDa), relatively high Gd content range (6.3–11.0%, w/w) compared to a reported prototype macromolecular contrast medium, albumin-(Gd-DTPA) $_{20-35}$ (4–6%).²¹ The number of attached Gd-DTPA per conjugate was 8.3, 7.5, 8.0, and 12.9 for compounds **1–4**, respectively. Structural and physicochemical information are given in Table 2. HP-SEC curves of PEG6000, PEG6000-Gen4, and PEG6000-Gen4-(Gd-DTPA) $_8$ from the same column are reproduced in Figure 3, showing that the sizes of the macromolecules in all stages of synthesis were narrowly distributed and that the introduction of PEG substan-

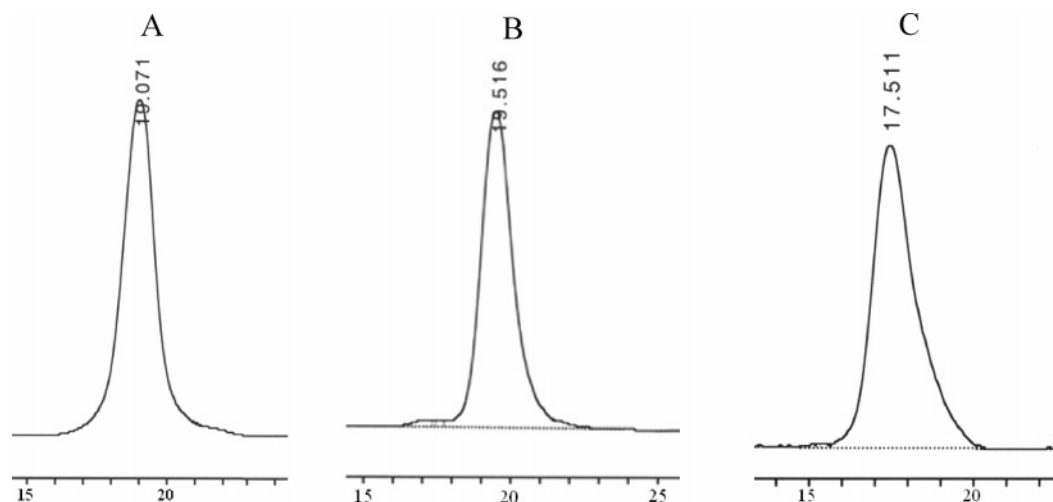


Figure 3. SE-HPLC traces of PEG6000 (A), PEG6000-Gen4 cascade polymer (B), and PEG6000-Gen4-(Gd-DTPA)₈ conjugate (C) on a Superdex 200 column with a flow rate of 0.8 mL/min, 30 min for each run, with refractive index (RI) detection for curve A and UV detection for curves B and C at 210 nm. Mobile phases: for A and C, 0.05 M phosphate and 0.15 M NaCl (pH 7.0); for B, 0.1% trifluoroacetic acid and 0.3 M Na₂SO₄ (pH 2.7).

Table 4. T₁ Relaxivities (mM⁻¹ s⁻¹) of PEG-Core Macromolecular Contrast Media under Varying Conditions (Medium, Temperature, and Magnetic Field)

contrast medium	in 0.1 M HEPES buffer (pH 7)				in rat plasma 37 °C, 0.25 T
	23 °C		37 °C		
	0.25 T	2 T	0.25 T	2 T	
PEG3400-Gen4-(Gd-DTPA) ₈	8.29	7.25	8.42	8.12	8.40
PEG6000-Gen4-(Gd-DTPA) ₈	8.64	8.59	8.72	9.76	8.80
PEG12000-Gen4-(Gd-DTPA) ₈	8.12	7.87	8.56	8.88	8.59
PEG3400-Gen5-(Gd-DTPA) ₁₃	10.10	8.60	10.68	9.52	10.58
albumin-(Gd-DTPA) ₃₅	11.48	9.07	10.44	10.09	nd ^a
Gd-DTPA	5.55	4.29	5.11	2.90	nd

^a Not determined.

tially contributed to the effective size of this contrast-enhancing macromolecule **2**.

Physical Characteristics. Proton T₁ Relaxivity. At 0.25 T, all three Gen4 cascade conjugates evaluated in this study showed similar, relatively high T₁ relaxivities, between 8 and 9 mM⁻¹ s⁻¹ (Table 4). The rank order of T₁ relaxivity measurements remained the same at physiological (37 °C) and room (23 °C) temperatures, as follows: Gd-DTPA < Gen4 conjugates < Gen5 conjugate < albumin-(Gd-DTPA)₃₅. In comparison to a single Gd-DTPA complex, increases of 50–82% and 65–109% were found for the PEG-core contrast media at 23 and 37 °C, respectively.

Of importance, the observed absence of change in T₁ relaxivities for PEG-core contrast media between an aqueous pH buffer solution and rat plasma supports the conclusion of a lack of plasma protein binding by this class of PEG-core cascade polymer contrast media (Table 4).

At 2.0 T (Table 4) and 37 °C, PEG-core contrast media had relaxivities 3.1–3.4 times the relaxivity value of unbound Gd-DTPA but approximately 1× of the T₁ relaxation effect of Gd in macromolecular albumin-(Gd-DTPA)₃₅. These observations are consistent with a slowing of the rotational correlation rate with Gd-chelate incorporation into macromolecular compounds causing an increase in relaxation effectiveness of each Gd-containing complex of the macromolecular species.^{22,23} Also, a moderate increase (up to 25% and 17%) of T₁ relaxivity was observed in the Gen5 polymer compared to that of the Gen4 polymer at 0.25 and 2 T, respectively.

Worthy of mention, T₁ relaxivities of all Gd-DTPA conjugated cascade macromolecules had a positive temperature

dependence within the range of 23 to 37 °C at both 0.25 and 2.0 T fields. This is similar to previously observed characteristics of DTPA amides, implying that the T₁ relaxivities of these highly hydrophilic polymer conjugates with Gd-DTPA monoamides were probably limited by the water exchange rate.²⁴

Hydrophilicity and Osmolality. Table 2 shows that the measured butanol–water partition coefficients for PEG-core contrast media were 1 × 10⁻⁵, or less, even lower than the value for clinically approved Gd-DTPA (2 × 10⁻⁵) and only 1/28 of the measured value for albumin-(Gd-DTPA)₃₅. These results indicating that the PEG-core cascade polymeric contrast media were more hydrophilic than both a prototype protein-based MRI contrast medium and the clinically used Gd-DTPA complex are likely attributable to the highly hydrophilic PEG cores. Osmolality measurements for 0.1 M solutions of all synthesized compounds (Table 2) ranged from ~390 to 600 mOsm/kg, about 50–75% of the measured value for albumin-(Gd-DTPA)₃₅ at the same Gd concentration. This difference in osmotic effect possibly resulted from the nonionic character of the PEG backbone compared to the more ionic nature of albumin. The osmolality of compound **4** (Gen5 polymer) is found to be moderately higher than that of compounds **1–3** (Gen4 polymers); this could be due to its higher number of net molecular charge.

Chelate Stability, Stability in Plasma, and Stability to Autoclaving Conditions. Thermodynamic stability of one representative conjugate was measured according to an established competitive chelation method (Table 2). According to this method UV spectrometry is employed to determine the competitive chelation equilibrium between Gd–arsenazo III chelates

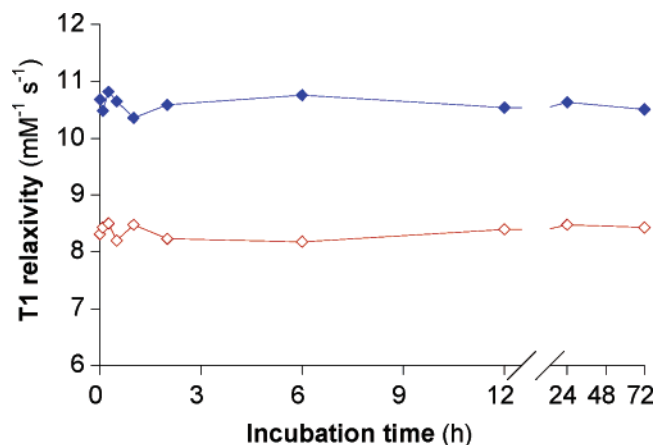


Figure 4. In vitro stabilities of PEG3400-Gen4-(Gd-DTPA)₈ (◇) and PEG3400-Gen5-(Gd-DTPA)₁₃ (◆) in rat plasma (37 °C) monitored by relaxometry over 3 days.

(both 1:1 and 1:2 chelates) and our representative macromolecular ligands, PEG6000-Gen4-DTPA and PEG3400-Gen5-DTPA. The log value of the thermodynamic stability constant for PEG6000-Gen4-(Gd-DTPA)₈ was 18.3 ± 0.2 , similar to the literature data (18.8 ± 0.1) reported by Sherry et al. for macromolecular Gd-DTPA-BSA.¹¹ Similar thermodynamic stability was found for PEG3400-Gen5-(Gd-DTPA)₁₃ (see Table 2). This may indicate that the chelate stability is hardly affected by the PEG size and cascade generation. Of further note, the conditional stability constants at physiological pH (7.4) were calculated to be 15.9 and 16.2 (log values) for compounds **2** and **4**, respectively, according to the same literature method.

The chelation stability for these synthesized contrast media are relatively high; however, we recognize that a DTPA monoamide chelate is lower in stability than a DTPA chelate due to one less chelating group. Macrocyclic aminocarboxylate ligands can generally be expected to provide more stability than open-chain aminocarboxylate ligands. Accordingly, we plan to improve the thermodynamic stability of subsequent candidate compounds by using a Gd-DOTA derivative.

As shown in Figure 4, the T1 relaxivity for PEG3400-Gen5-(Gd-DTPA)₁₃ was stable over 72 h when incubated in rat plasma at 37 °C. After 72 h of incubation, its relaxivity remained unchanged, about $10.5 \text{ mM}^{-1} \text{ s}^{-1}$. Similar chemical stability in plasma was observed for PEG3400-Gen4-(Gd-DTPA)₈ by relaxometry, with a relaxivity of about $8.4 \text{ mM}^{-1} \text{ s}^{-1}$. The stability of T1 relaxivity values in plasma suggests the chemical inertness of this type of contrast medium to the plasma enzymes and a lack of protein binding.

No change in SE-HPLC traces was found for the PEG3400-Gen5-(Gd-DTPA)₁₃ solution before and after heating to 120 °C for 30 min, typical autoclaving conditions (data not shown). This indicates an absence of heat-induced cross-linking or degradation of this macromolecule. Assuming this degree of stability can be generalized to the entire class of PEG-core MRI contrast media, the class could be considered autoclavable.

Blood Pharmacokinetics Assayed by Dynamic MR Imaging. The curves of blood proton T1 relaxation responses to each of the four new contrast media were acquired using T1-weighted dynamic MRI over an observation period of approximately 45 min (Figure 5). Measurements were made in regions of interest defined by the brightly enhancing blood within the inferior vena cava. The signal in the blood for the two larger macromolecules, as reflected in their molecular weights, **3** and **4**, decayed monoexponentially with half-lives of 36 and 73 min, respectively (Table 3). The two smaller macromolecules, **1** and **2**, showed

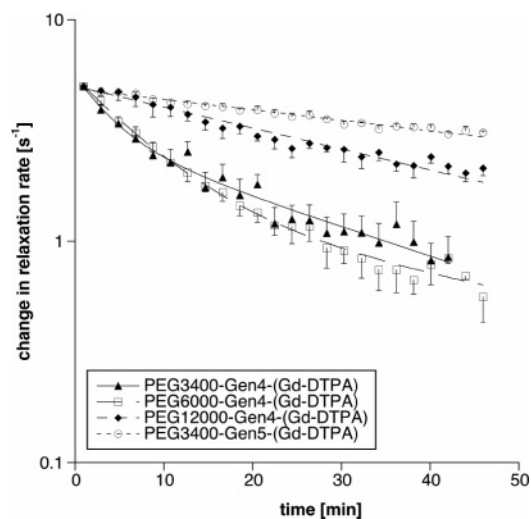


Figure 5. Plot of blood $\Delta(1/T_1)$, normalized to $5.0 \text{ mM}^{-1} \text{ s}^{-1}$ for first data points of each series over a 45 min period, acquired by MR imaging after intravenous administration of each PEG-core contrast medium. The value of $\Delta(1/T_1)$ is proportional to the Gd concentration under given experimental conditions. Each data point was presented as the mean and SD (animal number = 4 or 5 for each single group).

biexponential blood decay patterns. When the data from all four PEG-core contrast media are considered, blood half-lives ranged from 23 to 73 min, volumes of distribution (V_{ss}) were between 8.4% and 18%, and total clearance rates (CI) varied between 0.8 and $5.3 \text{ mL}/(\text{min} \cdot \text{kg})$. On the basis of the similar biexponential blood curves for the smaller conjugates, **1** and **2**, it was concluded that for Gd-DTPA conjugated generation-4 cascade polymers, the PEG6000 core is not large enough to yield a monoexponential blood response. A further increase in size, either in PEG core approaching 12 kDa or in generation number approaching Gen5, resulted in a preferred monoexponential blood enhancement curve. Furthermore, recognition of a desirable, longer blood half-life (1.2 h) and a smaller volume of distribution (8.4%, close to the typical physiological 5% fractional blood volume of most mammalian organisms), PEG3400-Gen5-(Gd-DTPA)₁₃ (compound **4**) distinguished itself in a favorable way from the other three compounds. In addition, the total clearance rates (CI) of these four contrast media decreased in the following order, **1** > **2** > **3** > **4**, while their blood half-lives increased in the same order. All four compounds behaved like intermediate or large molecular contrast media, in contrast to Gd-DTPA itself, while compounds **3** and **4** were close to the kinetics of a prototype blood pool MRI agent, albumin-(Gd-DTPA)₃₅.

Focusing on the influence of different generations, compounds **1** and **4**, both derived from PEG3400 core, had cascade generations of 4 and 5, respectively. The Gen5 conjugate persisted substantially longer (73 min) in the blood circulation than the Gen4 conjugate (<23 min); this might be explained by its more bulky cluster of lysines attached at either end of the PEG3400 core or by the calculated more positive charge of conjugate **4**. Interestingly, under in vitro conditions imposed by a Superdex 200 SEC column, compound **4** appeared to be smaller than PEG12000-Gen4-(Gd-DTPA)₈ (**3**), specifically, 106 versus 132 kDa in terms of the apparent molecular weight, while the in vivo blood half-life of compound **4** was considerably longer than **3**, specifically, 73 versus 36 min (monoexponential kinetics for both). Perhaps this seeming paradox of size and blood retention is due to differences in molecular charge or configuration. Compound **4** has more bulky and notably larger "cascade amplifiers" than **3** (Gen5 vs Gen4), which may slow

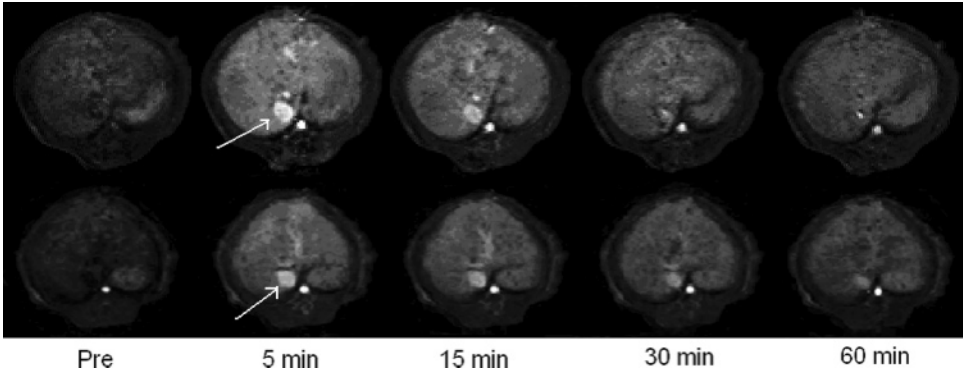


Figure 6. Representative enhancement kinetics as revealed by T1-weighted dynamic 3D MR imaging (spoiled gradient recalled sequence, SPGR) of a normal rat at the level of the liver after intravenous injection of PEG12000-Gen4-(Gd–DTPA)₈ (upper row) and PEG3400-Gen5-(Gd–DTPA)₁₃ (lower row), respectively, at a dose of 0.04 mmol Gd/kg. The blood enhancement as seen in the inferior vena cava is relatively prolonged being still visible for at least 30 and 60 min, respectively, for these two agents. Their monoexponential blood half-lives were calculated to be 36 and 73 min (mean values), respectively.

Table 5. Whole Body Retention Data for Two Representative Cascade Macromolecular Contrast Media with PEG Cores: PEG3400-Gen5-(Gd–DTPA)₁₃ and PEG12000-Gen4-(Gd–DTPA)₈

time	animal	dose % per organ, mean (SE) ^a				dose % per g of tissue, mean (SE) ^a			
		kidneys	liver	carcass	total	kidney	liver	carcass	total
PEG3400-Gen5-(Gd–DTPA) ₁₃									
1 week	<i>n</i> = 2	3.3 (0.5)	5.2 (0.7)	25.5 (1.5)	33.9 (2.7)	2.01 (0.20)	0.78 (0.06)	0.19 (0.02)	0.24 (0.02)
2 weeks	<i>n</i> = 1	1.9	4.1	19.8	25.8	1.06	0.56	0.13	0.16
PEG12000-Gen4-(Gd–DTPA) ₈									
2 weeks	<i>n</i> = 2	0.45 (0.02)	1.8 (0.1)	12.0 (0.5)	14.2 (0.4)	0.18 (0.01)	0.19 (0.01)	0.08 (0.01)	0.09 (0.005)
3 weeks	<i>n</i> = 1	0.32	1.2	9.6	11.1	0.14	0.10	0.06	0.06
Albumin-(Gd–DTPA) ₃₅ (literature data) ^b									
5 day	na ^c				60	na			
2 weeks	na				26	na			
3 weeks	na				21	na			

^a Standard error. ^b Reference 26. ^c Not available.

down the glomerular filtration process in renal clearance. Further, compound **4** has more net electric charges than **3** in both amplifiers; the intramolecular electric repulsion might make the cascade components even more extended and bulky, thus enhancing its slowing down of the renal filtration. One conclusion from these data is that higher effective molecular size measured by SEC does not completely predict a longer retention in blood. Essentially, the kinetic behavior of a macromolecule in blood is not solely dependent on molecular size but may be considerably influenced by molecular configuration and geometric conformation, the electric charge, and potential interactions with surrounding tissues.

As shown in Figure 6, the MRI enhancement of blood vessels (inferior vena cava) and highly vascular solid tissues such as liver induced by a PEG-core cascade polymer in the normal rat was both strong and persistent for 15 min or longer. For comparison, although not shown here, the MRI enhancement effect observable in blood after administration of Gd–DTPA (gadopentetate, MW 547 Da), a conventional commercially available extracellular fluid space (ECF) contrast medium, is exhausted in the rat by 2 min or less.²⁵ The macromolecular PEG-core cascade polymer-induced enhancement remains much longer in the blood and richly vascular soft tissues.

Whole Body Clearance. The two largest PEG-based macromolecules, **3** and **4**, were chosen for this bioelimination study that extended over a period of 3 weeks. Results are shown in Table 5. Highly sensitive Gd(III) detection techniques including

both ICP-MS and ICP-AES were employed to determine the Gd content of rat liver, kidneys, and remaining carcasses. For PEG3400-Gen5-(Gd–DTPA)₁₃, at the end of 1 week 3%, 5%, and 26% of the intravenously administered dose was recoverable, respectively, in the kidneys, liver, and remaining carcass. These residual values decreased further, indicating continued elimination, to 2%, 4%, and 20% at the end of the second week. The bodily elimination of this compound was similar to that reported by White et al. for albumin-(Gd–DTPA)₃₅.²⁶ Compound **3**, PEG12000-Gen4-(Gd–DTPA)₈, showed a substantially more rapid and complete bodily elimination than compound **4**; specifically, 0.5%, 1.8%, and 12% retention of the injected dose in the kidneys, liver, and carcass, respectively, after 14 days. By the end of the third week, 21 days, the levels of retained Gd(III) declined even further to 0.3%, 1.2%, and 9.6% for compound **3**. One can only speculate as to the extent of bioelimination had the observations been continued longer than 21 days. Yet the 3 week retention levels are notably lower than the 21% retention observed by White et al. for the albumin-based Gd–DTPA conjugate. The observed relatively high tissue retention may be further reduced by the use of thermodynamically more stable chelates.

Comparison of PEG-Core Polymer Characteristics with Previously Described MMCM. Macromolecular MRI contrast media can be classified into two major categories: polymer–Gd-chelate conjugates and polymer-stabilized iron oxide particles. This topic has recently been reviewed in detail by

Daldrup-Link and Brasch for those seeking an in-depth perspective.³ Certain iron oxide based MMCM, generally the smaller "ultrasmall" superparamagnetic iron oxide (USPIO) particles having total diameters of 10–30 nanometers, have been shown to be useful for defining quantitative MRI characteristics of cancers, including hypermeability to macromolecules.^{27,28} USPIO, as shown in a limited clinical trial,²⁹ are tolerated well in human patients despite the absence of a physiological means to eliminate iron or other metal ions from the body; the iron needs not to be excreted because it is thought to join the body's small normal iron pool used for hemoglobin synthesis.³⁰ However, USPIO particulate iron has not progressed far as a clinical contrast medium and USPIO have certain disadvantageous properties for cancer characterization including a strong T2* effect that dictates administration of only low doses when used for T1-weighted applications, typically necessary for quantitative tumor characterization. These low iron oxide doses yield unimpressive levels of tumor enhancement.³

Over the last 2 decades, some Gd-based polymeric MMCM have been proposed. Different obstacles or shortcomings have been encountered for each candidate with no currently described MMCM formulation meeting all requirements for clinical development. Large MMCM represented by albumin-(Gd-DTPA)₃₅ (MW ~92 kDa)²¹ or Gd-loaded polysaccharide (72 kDa)³¹ or dendritic constructs^{32,33} are considered useful or potentially useful to defining microvascular hypermeability of cancer and other disease states but are too large and metabolically inert to be adequately excreted from the body. Albumin-(Gd-DTPA)₃₀ and other protein-based MMCM also are potentially immunogenic.

Alternatively, some intermediately sized contrast media with molecular weights <50 kDa, e.g., Gadomer-17,^{34,35} P792^{34,36} are small enough for prompt bodily elimination by the kidney but are too small to optimally exploit and define the macromolecular hypermeability of cancer microvessels, a biological characteristic observed with molecules larger than 70 kDa. Other formulations are hindered by molecular polydispersity (e.g., Gd-DTPA-polylysine,³⁷ carboxymethyl-dextran-(Gd-DO3A)³⁸). Contrast media that exist in vivo in an equilibrium between protein-bound macromolecular species and unbound small molecular species (e.g., MS-325, B22956/1)^{39,40} are problematic because the kinetics and thus the permeabilities for the different species cannot be easily deconvoluted.

Certain cascade polymeric contrast media were reported previously, including, e.g., Gd-loaded polyamidoamine (PAM-AM) starburst polymers,⁴¹ pegylated Gd-DTPA-PAMAM,⁴² and Gd-loaded polypropylenimine cascade polymers.⁴³ The new class of PEG-core contrast media reported here differs from these by having a PEG core centrally located within the structure, and by using L-lysine as the monomer unit of the cascade amplifiers. In previous studies of PEG-containing MMCM, PEG has been introduced, without exception, to either side chains of linear macromolecules (e.g., poly-L-lysine) or to surface groups of hyperbranched macromolecules in a straightforward, however less controllable, manner since the number of attached PEG was essentially uncertain in the pegylation step. In our design, we have introduced PEG into the cascade polymer as an initiating core; thus, both the number and site of introduced PEGs (one) is well defined for all generations.

Our initially reported PEG-core Gd-based contrast media exhibited high T1 relaxivity (up to 3-fold compared to a single Gd-DTPA at a clinically used magnetic field of 2 T), considerably high Gd content, narrow size dispersity, high hydrophilicity, lack of protein binding, prolonged blood half-

life (up to 73 min with monoexponential kinetics) with actual molecular weights as low as 12–20 kDa, and autoclaving stability. Their blood pharmacokinetics could be tuned by adjusting the PEG core size, the generation number of the cascades, and the number and electric charge of the attached individual Gd chelate. This is the first in vivo evaluation of this interesting and new class of dumbbell-like cascade polymers with a PEG core, intended for MR imaging applications.

However these initially reported PEG-core polymer amplifiers had only modest degrees of conjugation (20–25% of total potential) with Gd-DTPA. Other specific characteristics observed for these initial series of PEG-core cascade polymeric contrast media that encourage further attention include thermodynamic chelation stability ($\log K = 18.3$) and bodily elimination (11% retention at 3 weeks). Raising the thermodynamic stability to levels higher than 22 and increasing total body elimination to 99% or better should yield greater safety and acceptably low gadolinium retention. A further development along this line is to substitute these PEG-core polymer amplifiers more completely with different types of even more stable Gd chelates.

Conclusion

To summarize, candidate compounds from a new class of PEG-core cascade polymers, conjugated with Gd-DTPA chelates, were synthesized and demonstrated characteristics, many being favorable for further development as diagnostic MRI macromolecular contrast media. A threshold of effective molecular size for obtaining a monoexponential blood clearance in tested animals was determined between 82 and 106 kDa effective molecular weight. Current results should prove helpful in the refinement and further development of this drug class.

Acknowledgment. This work was supported by NIH Grants CA103850 and CA82923. MALDI-TOF MS measurements were conducted by the UCSF Mass Spectrometry Facility (NIH NCRN RR01614). ¹H NMR spectra were recorded on a Varian 400 NMR spectrometer in the NMR Lab, UCSF School of Pharmacy at UCSF. Dr. Timothy P. L. Roberts is thanked for his helpful discussions. Dr. Mark Knudsen is thanked for his assistance in the relaxivity measurement.

References and Notes

- Gries, H. Extracellular MRI contrast agents based on gadolinium. In *Topics in Current Chemistry*; Springer: Berlin, 2002; Vol. 221, pp 1–24.
- Clarkson, R. B. Blood-pool MRI contrast agents: properties and characterization. In *Topics in Current Chemistry*; Springer: Berlin, 2002; Vol. 221, pp 201–235.
- Daldrup-Link, H. E.; Brasch, R. C. *Eur. Radiol.* **2003**, *13*, 354–365.
- Kobayashi, H.; Brechbiel, M. W. *Adv. Drug Delivery Rev.* **2005**, *57*, 2271–2286.
- Fu, Y.; Nitecki, D. E.; Maltby, D.; Simon, G. H.; Berejnoi, K.; Raatschen, H. J.; Yeh, B. M.; Shames, D. M.; Brasch, R. C. *Bioconjugate Chem.* **2006**, *17*, 1043–1056.
- Habeeb, A. F. S. A. *Anal. Biochem.* **1966**, *14*, 328–336.
- Nevins Buchanan, S. A.; Balogh, L. P.; Meyerhoff, M. E. *Anal. Chem.* **2004**, *76*, 1474–1482.
- Schmiedl, U.; Ogan, M. D.; Moseley, M. E.; Brasch, R. C. *Am. J. Roentgenol.* **1986**, *147*, 1263–1270.
- Turetschek, K.; Preda, A.; Floyd, E.; Shames, D. M.; Novikov, V.; Roberts, T. P.; Wood, J. M.; Fu, Y.; Carter, W. O.; Brasch, R. C. *Eur. J. Nucl. Med. Mol. Imaging* **2003**, *30*, 448–455.
- Krause, W.; Schuhmann-Giampieri, G.; Bauer, M.; Press, W. R.; Muschick, P. *Invest. Radiol.* **1996**, *31*, 502–511.
- Sherry, A. D.; Cacheris, W. P.; Kuan, K. T. *Magn. Reson. Med.* **1988**, *8*, 180–190.

- (12) Daldrup, H.; Shames, D. M.; Wendland, M.; Okuhata, Y.; Link, T. M.; Rosenau, W.; Lu, Y.; Brasch, R. C. *Am. J. Roentgenol.* **1998**, *171*, 941–949.
- (13) Roberts, T.; Schwickert, H.; Brasch, R. Proceedings of the International Society of Magnetic Resonance in Medicine (ISMRM) the 3rd Scientific Meeting, Nice, France, August 19–25, 1995; p 1129.
- (14) Vexler, V. S.; Clement, O.; Brasch, R. C. *Invest. Radiol.* **1994**, *29* (Suppl. 2), S62–64.
- (15) Frame, E. M. S.; Uzgiris, E. E. *Analyst* **1998**, *123*, 675–679.
- (16) Harris, J. M. *Poly(ethylene glycol) Chemistry: Biotechnical and Biomedical Applications*; Plenum Press: New York, 1992.
- (17) Duncan, R. *Nat. Rev. Drug Discovery* **2003**, *2*, 347–360.
- (18) Delgado, C.; Francis, G.; Fisher, D. *Crit. Rev. Ther. Drug Carrier Syst.* **1992**, *9*, 249–304.
- (19) Choi, J. S.; Lee, E. J.; Choi, Y. H.; Jeong, Y. J.; Park, J. S. *Bioconjugate Chem.* **1999**, *10*, 62–65.
- (20) Choi, J. S.; Joo, D. K.; Kim, C. H.; Kim, K.; Park, J. S. *J. Am. Chem. Soc.* **2000**, *122*, 474–480.
- (21) Ogan, M.; Schmiedl, U.; Moseley, M.; Grodd, W.; Paajenen, H.; Brasch, R. C. *Invest. Radiol.* **1987**, *22*, 665–671.
- (22) Koenig, S. H. *Invest. Radiol.* **1994**, *29*, S127–S130.
- (23) Caravan, P.; Ellison, J. J.; McMurry, T. J.; Lauffer, R. B. *Chem. Rev.* **1999**, *99*, 2293–2352.
- (24) Geraldes, C. F.; Urbano, A. M.; Alpoim, M. C.; Sherry, A. D.; Kuan, K. T.; Rajagopalan, R.; Maton, F.; Muller, R. N. *Magn. Reson. Imaging* **1995**, *13*, 401–420.
- (25) Brasch, R. C.; Weinmann, H. J.; Wesbey, G. E. *Am. J. Roentgenol.* **1984**, *142*, 625–630.
- (26) White, D. L.; Wang, S. C.; Aicher, K. P.; Dupon, J. W.; Engelstad, B. L.; Brasch, R. C. Proceedings of the SMRM Eighth Annual Meeting, Amsterdam, Aug 12–18, 1989; p 807.
- (27) Jain, R. *Sci. Am.* **1994**, *271*, 58–65.
- (28) Turetschek, K.; Roberts, T.; Floyd, E.; Preda, A.; Novikov, V.; Shames, D.; Carter, W. O.; Brasch, R. *J. Magn. Reson. Imaging* **2001**, *13*, 882–888.
- (29) Daldrup-Link, H. E.; Rydland, J.; Helbich, T. H.; Bjornerud, A.; Turetschek, K.; Kvistad, K. A.; Kaindl, E.; Link, T. M.; Staudacher, K.; Shames, D.; Brasch, R. C.; Haraldseth, O.; Rummeny, E. J. *Radiology* **2003**, *229*, 885–892.
- (30) Bulte, J. W. M.; Brooks, R. A. Magnetic nanoparticles as contrast agents for MR imaging. In *Scientific and Clinical Applications of Magnetic Carriers*; Haefeli, U., Schuett, W., Teller, J., Zborowski, M., Eds.; Plenum Press: New York, 1997; pp 527–543.
- (31) Helbich, T. H.; Gossman, A.; Mareski, P. A.; Raduchel, B.; Roberts, T. P. L.; Shames, D.; Muhler, M.; Turetschek, K.; Brasch, R. C. *J. Magn. Reson. Imaging* **2000**, *11*, 694–701.
- (32) Aref, M.; Brechbiel, M.; Wiener, E. C. *Invest. Radiol.* **2002**, *37*, 178–192.
- (33) Kobayashi, H.; Brechbiel, M. W. *Curr. Pharm. Biotechnol.* **2004**, *5*, 539–549.
- (34) Dong, Q.; Hurst, D. R.; Weimann, H. J.; Chenevert, T. L.; Londy, F. J.; Prince, M. R. *Invest. Radiol.* **1998**, *33*, 699–708.
- (35) Daldrup-Link, H. E.; Shames, D. M.; Wendland, M.; Okuhata, Y.; Muhler, A.; Gossman, A.; Rosenau, W.; Brasch, R. C. *Acad. Radiol.* **2000**, *7*, 934–944.
- (36) Turetschek, K.; Floyd, E.; Shames, D. M.; Roberts, T. P. L.; Preda, A.; Novikov, V.; Corot, C.; Carter, W. O.; Brasch, R. C. *Magn. Reson. Med.* **2001**, *45*, 880–886.
- (37) Schuhmann-Giampieri, G.; Schmitt-Willich, H.; Frenzel, T.; Press, W. R.; Weinmann, H. J. *Invest. Radiol.* **1991**, *26*, 969–997.
- (38) Kroft, L. J.; Doornbos, J.; van der Geest, R. J.; de Roos, A. J. *Magn. Reson. Imaging* **1999**, *10*, 170–177.
- (39) Turetschek, K.; Floyd, E.; Helbich, T. H.; Roberts, T. P. L.; Shames, D. M.; Wendland, M. F.; Carter, W. O.; Brasch, R. C. *J. Magn. Reson. Imaging* **2001**, *14*, 237–242.
- (40) Cavagna, F. M.; Lorusso, V.; Anelli, P. L.; Maggioni, F.; de Haen, C. *Acad. Radiol.* **2002**, *9* (suppl. 2), S491–494.
- (41) Wiener, E. C.; Brechbiel, M. W.; Brother, H.; Magin, R. L.; Gansow, O. A.; Tomalia, D. A.; Lauterbur, P. C. *Magn. Reson. Med.* **1994**, *31*, 1–8.
- (42) Kobayashi, H.; Kawamoto, S.; Saga, T.; Sato, N.; Hiraga, A.; Ishimori, T.; Konishi, J.; Togashi, K.; Brechbiel, M. W. *Magn. Reson. Med.* **2001**, *46*, 781–788.
- (43) Kobayashi, H.; Kawamoto, S.; Saga, T.; Sato, N.; Hiraga, A.; Ishimori, T.; Akita, Y.; Mamede, M. H.; Konishi, J.; Togashi, K.; Brechbiel, M. W. *Magn. Reson. Med.* **2001**, *46*, 795–802.
- (44) Weinmann, H. J.; Brasch, R. C.; Press, W. R.; Wesbey, G. E. *Am. J. Roentgenol.* **1984**, *142*, 619–624.
- (45) Vexler, V. S.; Clement, O.; Schmitt-Willich, H.; Brasch, R. C. *J. Magn. Reson. Imaging* **1994**, *4*, 381–388.

BM061141H